618 *Biochemistry* **2011,** *50,* 618–627
DOI: 10.1021/bi102046h

BIOCHEMISTRY
including biophysical chemistry & molecular biology
Article

Effect of the Thymidylate Synthase Inhibitors on dUTP and TTP Pool Levels and the Activities of DNA Repair Glycosylases on Uracil and 5-Fluorouracil in DNA†

Breeana C. Grogan, Jared B. Parker, Amy F. Guminski, and James T. Stivers*

Department of Pharmacology and Molecular Sciences, The Johns Hopkins University School of Medicine, 725 North Wolfe Street, Baltimore, Maryland 21205-2185, United States

Received December 22, 2010

ABSTRACT: 5-Fluorouracil (5-FU), 5-fluorodeoxyuridine (5-dUrd), and raltitrixed (RTX) are anticancer agents that target thymidylate synthase (TS), thereby blocking the conversion of dUMP into dTMP. In budding yeast, 5-FU promotes a large increase in the dUMP/dTMP ratio leading to massive polymerase-catalyzed incorporation of uracil (U) into genomic DNA, and to a lesser extent 5-FU, which are both excised by yeast uracil DNA glycosylase (UNG), leading to DNA fragmentation and cell death. In contrast, the toxicity of 5-FU and RTX in human and mouse cell lines does not involve UNG, but, instead, other DNA glycosylases that can excise uracil derivatives. To elucidate the basis for these divergent findings in yeast and human cells, we have investigated how these drugs perturb cellular dUTP and TTP pool levels and the relative abilities of three human DNA glycosylases (hUNG2, hSMUG1, and hTDG) to excise various TS drug-induced lesions in DNA. We found that 5-dUrd only modestly increases the dUTP and dTTP pool levels in asynchronous MEF, HeLa, and HT-29 human cell lines when growth occurs in standard culture media. In contrast, treatment of chicken DT40 B cells with 5-dUrd or RTX resulted in large increases in the dUTP/TTP ratio. Surprisingly, even though UNG is the only DNA glycosylase in DT40 cells that can act on U·A base pairs derived from dUTP incorporation, an isogenic *ung*$^{-/-}$ DT40 cell line showed little change in its sensitivity to RTX as compared to control cells. In vitro kinetic analyses of the purified human enzymes show that hUNG2 is the most powerful catalyst for excision of 5-FU and U regardless of whether it is found in base pairs with A or G or present in single-stranded DNA. Fully consistent with the in vitro activity assays, nuclear extracts isolated from human and chicken cell cultures show that hUNG2 is the overwhelming activity for removal of both U and 5-FU, despite its bystander status with respect to drug toxicity in these cell lines. The diverse outcomes of TS inhibition with respect to nucleotide pool levels, the nature of the resulting DNA lesion, and the DNA repair response are discussed.

The antimetabolites 5-fluorouracil (5-FU),[1] 5-fluorodeoxyuridine (5-dUrd), and raltiterxed (RTX) are widely used for the treatment of colorectal, breast, and head and neck cancers (*1*−*3*). Fluoropyrimidines are metabolized much like uracil and deoxyuridine and can be enzymatically converted to the active metabolite 5-FdUMP (Figure 1). A binary complex between 5-FdUMP and 5,10-methylenetetrahydrofolate irreversibly inhibits thymidylate synthase (TS), blocking de novo production of dTMP and also resulting in the accumulation of dUMP. The resulting thymine nucleotide pool deficiency caused by fluoropyrimidine drugs was originally thought to induce the therapeutic effect by a process called "thymineless death". However, an additional hallmark of fluoropyrimidine treatment is the polymerase-catalyzed incorporation of dUMP and 5-F-dUMP into DNA, resulting in U·A, 5-FU·A, and 5-FU·G base pairs that are substrates for various uracil DNA repair glycosylases (*1*, *4*, *5*). Similarly, RTX is a TS-specific folate mimic that also prevents TMP synthesis, but unlike fluoropyrimidines, RTX results in the accumulation of only dUMP and U·A base pairs in DNA. Thus, the toxicity mechanisms of these drugs will depend on the dUTP, 5-F-dUTP, and TTP pool levels, as well as the relative specificities of the cellular uracil DNA glycosylase activities toward these uracil-containing base pairs.

Several previous studies have investigated which DNA glycosylase enzymes are responsible for excising uracil and 5-FU bases in the context of U·A, 5-FU·A, and 5-FU·G base pairs and which are responsible for the toxic effects of the drug (*6*−*11*). In a study performed in budding yeast, Seiple and co-workers showed that deletion of the base excision repair enzyme uracil DNA glycosylase (UNG) resulted in a huge accumulation of U in the yeast genome during treatment with 5-FU (~4% of genomic thymidine levels), and that *ung*$^{-}$ yeast were protected against the

†This work was supported by Grant GM056834 from the National Institutes of Health to J.T.S. and a Ruth L. Kirschstein National Research Service Award (F31 GM083623) to J.B.P.

*To whom correspondence should be addressed: Department of Pharmacology and Molecular Sciences, The Johns Hopkins University School of Medicine, 725 N. Wolfe St., Baltimore, MD 21205-2185. Telephone: (410) 502-2758. Fax: (410) 955-3023. E-mail: jstivers@jhmi.edu.

[1]Abbreviations: DMEM, Dulbecco's modified Eagle's medium; RPMI, Roswell Park Memorial Institute medium; CM, chicken medium; LF-CM, low-folate chicken medium; SMUG1, single-strand selective monofunctional uracil DNA glycosylase; UNG2, nuclear uracil DNA glycosylase; TDG, thymine DNA glycosylase; TS, thymidylate synthase; dUTP, deoxyuridine triphosphate; 5-F-dUTP, 5-fluorodeoxyuridine triphosphate; dTTP, deoxythymidine triphosphate; 5-FU, 5-fluorouracil base; U, uracil; MEF, mouse embryonic fibroblast; MBD4, methyl-CpG-binding domain protein 4; FAM, 6-carboxyfluorescein; PBS, phosphate-buffered saline; PMSF, phenylmethanesulfonyl fluoride; DTT, dithiothreitol; PCA, phenol/chloroform/isoamyl alcohol mixture; BSA, bovine serum albumin; UGI, uracil DNA glycosylase inhibitor protein.

 Published on Web 12/28/2010

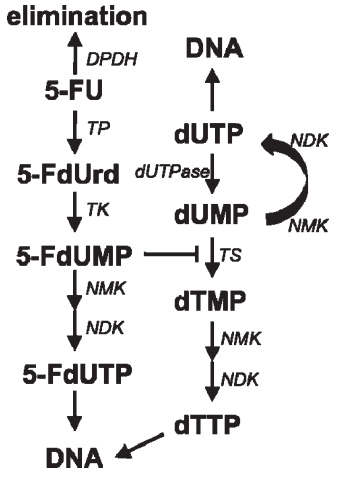

FIGURE 1: Pathways of 5-FU metabolism and DNA toxicity. Metabolites are shown in bold and enzymes in italics: **5-FU**, 5-fluorouracil; **5-FdUrd**, 5-fluorodeoxyuridine; **5-FdUMP**, 5-fluorodeoxyuridine monophosphate; **5-F-dUTP**, 5-fluorodeoxyuridine triphosphate; **dUTP**, deoxyuridine triphosphate; **dUMP**, deoxyuridine monophosphate; **dTMP**, deoxythymidine monophosphate; **dTTP**, deoxythymidine triphosphate; *TP*, thymidine phosphorylase; *NMK*, nucleotide monophosphate kinase; *NDK*, nucleotide diphosphate kinase; *TK*, thymidine kinase; *dUTPase*, dUTP nucleotide hydrolase; *TS*, thymidylate synthase; *DPDH*, dihydropyrimidine dehydrogenase.

cytotoxic effects of 5-FU (*8*). This study thus established two mechanistic aspects of 5-FU toxicity in the yeast system: (i) 5-FU treatment results in an elevated dUTP level and accumulation of U in genomic DNA, and (ii) 5-FU toxicity is dependent on excision of U by yeast UNG (UNG is the only enzyme in yeast that removes uracil from DNA).

In contrast to the findings with yeast, 5-FU toxicity studies using ung^+/ung^+ and ung^-/ung^- mouse embryonic fibroblasts (MEFs) indicated that UNG was not involved in the toxicity mechanism (*7*, *9*). Because there are four different DNA glycosylases in both mice and humans capable of excising U and 5-FU from DNA (UNG, SMUG1, TDG, and MBD4[2] /MED1) (*12*), it is perhaps not surprising that the role of yeast UNG could be supplanted by the combined activities of SMUG1 and TDG in MEF cells (*9*, *10*). From these combined studies, distinct roles for UNG, TDG, and SMUG were suggested. UNG was thought to have no role in preventing or precipitating the toxic effects of 5-FU in MEFs (*7*, *9*), a conclusion also obtained in another study using RTX and HEK293 cells (*13*). In the MEF cell studies, the glycosylase activity of TDG precipitated 5-FU toxicity in a manner analogous to that of UNG in yeast, while excision of 5-FU and U by SMUG1 was thought to protect cells against 5-FU toxicity.

To improve our understanding of these complex findings, we now examine the extent to which fluoropyrimidines and RTX alter the dUTP and TTP nucleotide pools in human, mouse, and DT40 chicken cells, and we measure the specific activities of DNA glycosylases hUNG2, hSMUG1, and hTDG against the diverse lesions that are generated from these drugs. In human and mouse cells, we find only small increases in the dUTP/TTP ratio after drug treatment in standard medium, but much larger increases using dialyzed medium that is depleted of folate and thymidine. Thus, previous studies using standard media may not have induced high dUTP levels, and consequently, incorporation of genomic uracil during the S phase would have been limited. In contrast, 5-FdUrd and RTX induce a large increase in the dUTP/TTP ratio in DT40 chicken cells. Despite UNG being the only U·A glycosylase activity in DT40 cells, the chicken UNG was found to provide no protective effect against the toxic effects of RTX, similar to results with human cells. Although UNG action is curiously irrelevant to drug toxicity in both human and chicken cells (vide supra), in vitro kinetic analyses of purified hUNG2, hSMUG1, and hTDG, as well as activity measurements using nuclear extracts, established that hUNG2 is paradoxically the primary cellular activity that removes U and 5-FU from DNA. We suggest that human and chicken cells are tolerant to U·A base pairs at the density at which they are introduced during drug treatment, and that the repair activity of UNG during the S phase is masked by this tolerance. The UNG-independent toxicity of the TS drugs with DT40 cells indicates that the killing mechanism is independent of both uracil base excision repair and mismatch repair (which acts on 5-FU·G base pairs).

[2]While the remaining 5-FU DNA glycosylase, MBD4, has been shown to excise 5-FU opposite G in vitro (*35*, *36*), it has yet to be implicated in 5-FU excision in vivo in either mouse or human cell lines (*14*, *27*).

EXPERIMENTAL PROCEDURES

Cloning, Expression, and Purification of hUNG2, hTDG, and hSMUG1. The gene for full-length hUNG2 (939 bp) was amplified from cDNA from the Invitrogen Ultimate ORF collection (clone IOH43486). The gene for hSMUG1 was obtained from GenScript (813 bp). Both genes were ligated into a pET-19b vector (Novagen), and sequences were confirmed by sequencing both DNA strands. Both proteins were expressed as N-terminal His_{10} fusions whose expression and purification protocols were identical. *Escherichia coli* C41 cells (Lucigen) were transformed with the pET-19b plasmid dsDNA and grown in LB medium at 37 °C. Once OD_{600} reached 0.6, the temperature was lowered to 25 °C and expression was induced via addition of 1 mM IPTG. After expression at 25 °C for 5 h, cells were harvested via centrifugation (4000*g*) and resuspended in lysis buffer containing 50 mM NaH_2PO_4 (pH 7.5), 500 mM NaCl, 0.1% Triton X-100, and 20 mM imidazole. Cells were lysed with a microfluidizer reaching ~20000 psi. The resulting cell lysate was clarified via centrifugation (40000*g*) and the supernatant loaded onto Ni-NTA resin (Qiagen) at 4 °C. The unbound protein was washed away with lysis buffer, and bound protein was eluted with lysis buffer containing 500 mM imidazole. Eluted protein was dialyzed into 20 mM Hepes-OH (pH 8.0), 200 mM NaCl, 0.1 mM EDTA, and 2 mM DTT, and the His_{10} tag was removed via protease. Crude protein was then dialyzed against buffer A [20 mM Hepes-OH (pH 8.0), 50 mM NaCl, 1 mM DTT, 0.1 mM EDTA, and 5% glycerol] and loaded onto a SP-Sepharose FF cation-exchange column (GE Healthcare). Bound protein was eluted with a 0 to 100% linear gradient of buffer A with 1 M NaCl. Fractions were analyzed via SDS−PAGE (Coomassie blue staining) and judged to be ~99% pure for both hUNG2 and hSMUG1. Protein mass was verified using MALDI-TOF mass spectrometry. Pure protein was dialyzed into storage buffer [20 mM Hepes-OH (pH 7.5), 100 mM NaCl, 0.2 mM EDTA, 1 mM DTT, and 10% glycerol], flash-frozen, and stored at −80 °C. Purified recombinant human TDG was a gift of A. Drohat (*14*, *15*).

DNA Substrates. All 5′-FAM-containing oligonucleotides were synthesized on an Applied Biosystems 394 DNA synthesizer using standard phosphoramidites and supports obtained from Glen Research as previously described (*16*). Unlabeled oligonucleotides were obtained from Integrated DNA Technologies.

Steady-State Kinetics. hUNG2 and hSMUG1 kinetics experiments were conducted at room temperature (~22 °C) in HEMN buffer [20 mM Hepes-OH (pH 7.5), 100 mM NaCl, 2.5 mM $MgCl_2$, 0.2 mM EDTA, 1 mM DTT, and 0.1 mg/mL BSA] under conditions where [E] ≪ K_m with titrated [S]. Reactions were run for 5−30 min and were quenched by addition of an equal volume of a 25/24/1 phenol/chloroform/isoamyl alcohol mixture (PCA) and vortexing. To process the reaction mixtures, an aliquot of the aqueous layer (containing the DNA) was then extracted and the DNA backbone cleaved at abasic sites via addition of 100 mM NaOH followed by heating at 95 °C for 10 min. Formamide was added to a final concentration of >95%, and the samples were subjected to 7 M urea−19% denaturing PAGE to separate full-length substrate (19-mer) from cleaved product (9-mer). The 5′-FAM label of the substrate and product was imaged in gel using a Typhoon imager (GE Healthcare) and quantitated using Quantity One (Bio-Rad). The reaction rate (k_{obs}) was plotted versus DNA substrate concentration, and kinetic parameters were determined by fitting the data to eq 1, where [S] is the substrate concentration, k_{cat} is the maximal reaction rate, and K_m is the substrate concentration at $^1/_2k_{cat}$.

$$k_{obs} = \frac{k_{cat}[S]}{K_m + [S]} \quad (1)$$

Single-Turnover Kinetics. Single-turnover kinetic experiments with hSMUG1 were performed manually at room temperature in HEMN buffer at [E] ≫ [S]. For slower reactions, experiments were performed by rapidly mixing equal volumes of enzyme and substrate using a hand-held pipet, and reactions were quenched via addition of an equal volume of 0.5 M HCl from a second pipet. For more rapid time courses, a rapid chemical quench-flow instrument was used (KinTek). An equal volume of 25/24/1 PCA was added to extract all the protein, and an aliquot of the aqueous layer (containing DNA) was removed for further processing. The DNA backbone was cleaved at abasic sites via addition of NaOH to obtain a pH of >10 followed by heating at 95 °C for 10 min. Substrate turnover was analyzed exactly as described for the steady-state measurements. The maximal single-turnover cleavage rate (k_{max}) was determined by plotting k_{obs} versus enzyme concentration ([E]) and fitting the data to eq 2, where K_D is [E] at $^1/_2k_{max}$.

$$k_{obs} = \frac{k_{max}[E]}{[E] + K_D} \quad (2)$$

Preparation of Nuclear and Total Cell Extracts. Mouse embryonic fibroblasts (MEF), HeLa cells, and HT-29 colon cancer cells were grown adherently at 37 °C in 5% CO_2 in either DMEM (MEF and HeLa) or RPMI (HT-29) medium supplemented with 10% fetal bovine serum and a 1% streptomycin/penicillin mixture. Cells were plated at ~20% confluence and allowed to grow for 48 h in the absence and presence of 1 μM 5-FU. Cells were then harvested by trypsinization and counted using a hemocytometer. Nuclear extracts were prepared from cells treated with 5-FU and untreated cells as previously described with slight modifications (*17*). Trypsinized cells were harvested via centrifugation at 200*g* and 4 °C and washed twice with 50 cell volumes of ice-cold PBS. All subsequent steps were performed at 4 °C. Pelleted cells were resuspended in 1 packed cell volume of buffer consisting of 10 mM Hepes-OH (pH 7.5), 10 mM NaCl, 1.5 mM $MgCl_2$, 0.5 mM PMSF, and 1 mM DTT, and cells were allowed to swell on ice for 15 min. Swollen cells were lysed by rapidly forcing them through a 25 5/8-gauge needle. Five passes were sufficient to obtain >95% cell lysis as judged via trypan blue staining under a light microscope. Crude nuclei were pelleted from the cell lysate via centrifugation at 800*g* for 5 min. This crude nucleus pellet was resuspended in $^2/_3$ packed cell volume (previously determined from the whole cell pellet) of buffer consisting of 20 mM Hepes-OH, 420 mM NaCl, 25% glycerol, 1.5 mM $MgCl_2$, 0.2 mM EDTA, 0.5 mM PMSF, and 1 mM DTT followed by incubation on ice for 30 min with gentle agitation. Insoluble debris was pelleted via centrifugation at 16000*g* for 5 min. The nuclear extract (supernatant) was dialyzed against 1000 volumes of buffer Z [20 mM Hepes-OH (pH 7.5), 100 mM NaCl, 2 mM EDTA, 1 mM DTT, 0.5 mM PMSF, and 5% glycerol] for 4 h at 4 °C using a 3500 Da molecular mass cutoff membrane (Pierce). Dialyzed extracts were flash-frozen and stored at −80 °C until they were used. Protein concentrations were determined using the Bradford assay (Bio-Rad) with BSA as the standard.

Cell extracts of DT40 $AID^{-/-}$ and $UNG^{-/-}AID^{-/-}$ chicken cells (a gift from P. J. Gearhart, National Institute of Aging, Bethesda, MD) were prepared from cells grown in suspension at 37 °C in 5% CO_2 in chicken cell medium [RPMI 1640, 10% fetal bovine serum (FBS), 1% chicken serum, 50 μM β-mercaptoethanol, and a 1% penicillin/streptomycin mixture]. Cells were plated at ~25% confluence and allowed to grow for 24 h in the absence and presence of either 7.5 μM 5-fluorodeoxyuridine (5-FdUrd) or 0.5 μM raltitrexed (RTX) in the presence of either chicken cell medium or folate-free chicken cell medium (folate-free RPMI 1640, 10% dialyzed FBS, 1% dialyzed chicken serum, 50 μM β-mercaptoethanol, 80 nM 5-methyl tetrahydrofolate, and a 1% penicillin/streptomycin mixture). After being incubated, cells were transferred to 15 mL Falcon tubes and spun down for 5 min at 1500 rpm and 4 °C. The supernatant was discarded, and the cells were washed with 1× PBS. Again, the supernatant was discarded, and the cells were resuspended in 125 μL of CelLytic M (Sigma). Cells were incubated, while being rocked, for 15 min at room temperature. Immediately following incubation, the cells were centrifuged for 15 min at 14000 rpm and 4 °C. The supernatant containing the soluble protein fraction was transferred to a prechilled Eppendorf tube. The concentration of each extract was determined by a Bradford assay (Bio-Rad) using BSA as a standard. Extracts were frozen and stored at −80 °C.

Base Excision Activity of Cell Extracts. For nuclear extracts prepared from human or mouse cells, activity assays were performed at 37 °C in nuclear extract buffer containing 20 mM Hepes-OH (pH 7.5), 100 mM NaCl, 2 mM EDTA, 1 mM DTT, and 0.1 mg/mL BSA. Nuclear extracts from untreated or 5-FU-treated cells (final concentration of 0.2 μg/μL in 20 μL) were preincubated at room temperature in the presence or absence of UGI (final concentration of 1 μM) for 20 min before initiation of the reaction by addition of the DNA substrate (final concentration of 1 μM). Aliquots of the reactions were quenched at 3 h by addition of an equal volume of 25/24/1 PCA and vortexing. Samples were processed and analyzed exactly as described for the steady-state experiments. For DT40 cell extracts, an extract volume containing 5 μg of total protein was added to TEN-X buffer [10 mM Tris-HCl (pH 7.5), 100 mM NaCl, 1 mM EDTA, and 0.2% Triton X-100], in the absence or presence of 1 μM UGI, and the reaction was initiated by the addition of 15 μL of fluorescent hairpin DNA substrate (300 nM, final volume of 150 μL): 5′-FAM-GsCsAUUAAGAAG-$(PEG)_6$-CUUCUUAATsGsCs-DAB-3′. This sequence contains a polyethylene glycol linker, phosphorothioate linkages to block

exonuclease activities present in cell extracts, and a fluorescein (FAM) and dabcyl (DAB) fluorophore-quench pair. The removal of multiple uracils from U·A base pairs by UNG results in separation of the DNA strands and an increase in fluorescence due to the separation of the fluorophore-quench pair (*16*). After being mixed, the reaction solution was immediately placed in a fluorescence cuvette, and time-based acquisition of the fluorescence intensity at 520 nm was performed for 600 s with readings taken every 10 s (FluoroMax 3 fluorimeter) using an excitation wavelength of 494 nm (integration time of 2.5 s, excitation slit of 1 nm, and emission slit of 4 nm). The time courses were fitted using Prism, and the velocities (FU/s) were taken from the linear slopes after the initial lag phase that results from distributive cleavage of the uracil sites.

Single-Nucleotide Extension (SNE) Experiment for Measurement of Intracellular dUTP, 5-F-dUTP, and TTP Levels. MEF, HeLa, HT-29 colon cancer, DT40 AID$^{-/-}$, and DT40 AID$^{-/-}$UNG$^{-/-}$ colon cancer cells were grown as described above. dNTPs were prepared as previously described with some modifications (*18*). Prior to drug treatment, ~10^5 cells were plated in a final volume of 3 mL. After 72 h (HT-29 and HeLa cells) or 42 h (MEF and DT40 cells), the medium was changed. In half of the samples, the medium remained the same; in the other half, the medium was changed to folate-free DMEM (MEF and HeLa) or RPMI (HT-29) with 10% dialyzed FBS and a 1% penicillin/streptomycin mixture and supplemented with 80 nM 5-methyl tetrahydrofolate or folate-free chicken medium (DT40). Cells in each type of medium were left untreated or treated with 7.5 μM 5-FdUrd or 0.5 μM RTX. After incubation for 24 h, drug-containing medium was removed and cells were washed with their corresponding, drug-free medium and then allowed to incubate for an additional 2 h under the same incubation conditions. Following the second incubation, the medium was removed and 400 μL of cold 60% methanol was incubated in the wells for 1 h at 4 °C to extract the dNTPs from adherent cell lines. Suspension cell lines were first washed with 1× PBS, counted using a Scepter automated cell counter (Millipore), centrifuged at 1500 rpm for 5 min, and then resuspended in 400 μL of cold methanol to extract dNTPs. Following incubation, the liquid in the wells was removed and applied to a Microcon microcentrifuge filter with a molecular mass cutoff of 10 kDa and allowed to centrifuge at 14000 rpm for 15 min. dNTPs were stored at −20 °C and were stable for no more than 1 week. Two 75 μL aliquots of each dNTP extraction were evaporated to dryness. To one aliquot was added 40 μL of dUTPase buffer (34 mM Tris-HCl, pH 8.0; 10 mM $MgCl_2$; 0.5 mM EDTA; 0.25 mg/mL BSA) containing 20 ng of dUTPase. To the second aliquot was added 40 μL of dUTPase buffer without dUTPase. The samples were allowed to incubate at 37 °C for 20 min. Then, 60 μL of 100% methanol was added, and the samples were again evaporated to dyness under vacuum. To the dried down dNTPs was added 100 μL of SNE buffer [34 mM Tris-HCl (pH 8.0), 10 mM $MgCl_2$, 0.2 mM EDTA, and 0.25 mg/mL BSA] containing 32 nM FAM-labeled primer/template and 50 units of Moloney murine leukemia virus reverse transcriptase (NEB), and the mixture was allowed to incubate for 45 min at 42 °C. To specifically assess dUTP and TTP levels, a DNA primer/template sequence with a single adenine nucleotide overhang was used:

```
5'FAM-TGTTCTATGTTCATACACCACA-3'
   3'-ACAAGATACAAGTATGTGGTGTA-5'
```

Following incubation with the polymerase, 50 μL of formamide containing 0.25% xylene cyanol and bromophenol blue was added to each sample followed by incubation at 95 °C for 20 min. Twelve microliters of each sample was then applied to a 20% denaturing polyacrylamide gel containing 7 M urea at 15 W/gel and 45 °C for ~2 h to separate the unextended primer from the primer that was extended by a single thymidine or deoxyuridine nucleotide. Gels were imaged on a Typhoon imager (GE Healthcare). Control experiments were performed with dGTP, dCTP, and dATP to confirm that this template primer is specifically extended by TTP, dUTP, and 5-FdUTP

SNE Data Analysis. Single-nucleotide extension was quantified using Quantity One (Bio-Rad). Standard curves [generated in triplicate (see Figure S1 of the Supporting Information)] were obtained by measuring the percent extension of increasing concentrations of dUTP and TTP standards (Roche Diagnostics). After calculation of the mean and standard deviation of the three replicate measurements, a standard curve was generated using a second-order polynomial fit (GraphPad Prism). The average percent extension of the dNTPs isolated from the cell extracts was determined in triplicate and compared to these standard curves to determine the concentration of TTP or the concentration of dUTP and 5-F-dUTP in each sample. For each sample, the amount of TTP was calculated as the amount of extension observed after dUTPase pretreatment (both dUTP and 5-F-dUTP are substrates for dUTPase and the polymerase after treatment with 5-FdUrd, but only dUTP is a substrate after treatment with RTX). The concentration of dUTP and 5-F-dUTP was calculated as a difference, i.e., concentration of dUTP and 5-F-dUTP = extension before dUTPase treatment − extension after dUTPase pretreatment. Concentrations were converted to picomoles of dNTP per 1 million cells.

Toxicity of 5-FdUrd and RTX to DT40 Cells. DT40 AID$^{-/-}$ and AID$^{-/-}$UNG$^{-/-}$ were grown as described above. In a 96-well plate, cells were plated at a concentration of 50000 cells/well and brought up to a final volume of 90 μL in either chicken medium or folate-free chicken medium. Ten microliters of 10× drug stocks (made up in folate-free RPMI 1640) was added to each well in triplicate. Final drug concentrations were in the range from 10 pM to 10 μM. Cells were allowed to incubate for 72 h at 37 °C in 5% CO_2. Following incubation, 10 μL of 5 mg/mL MTT [3-(4,5-dimethylthiazol-2-yl)-2,5-diphenyltetrazolium bromide in 1× PBS] was added to the cells. Cells were allowed to incubate for an additional 4 h under the same conditions. During this time, formazan crystals formed and precipitated. After incubation, crystals were resuspended in 100 μL of resuspension buffer (2-propanol containing 10% Triton X-100 and 0.1 M HCl), and the absorbance was read on a plate reader at 570−650 nm. Triplicate measurements were averaged, and the standard error was determined. IC_{50} values were calculated from curve fitting to eq 3.

$$\% \text{ survival} = 100/(1 + [\text{drug}]/IC_{50}) \quad (3)$$

RESULTS

5-FdUrd Does Not Significantly Increase the dUTP Concentration in Human and Mouse Cell Lines in Standard Culture Media. We were curious why previous studies in mammalian cell lines found no role for UNG in the toxicity of 5-FdUrd in human cell cultures, even though UNG was shown to play a significant role in the toxicity of 5-FU in yeast (*8*). An important prerequisite event that influences the toxicity mechanism is the magnitude by which the [dUTP]/[TTP] ratio is increased

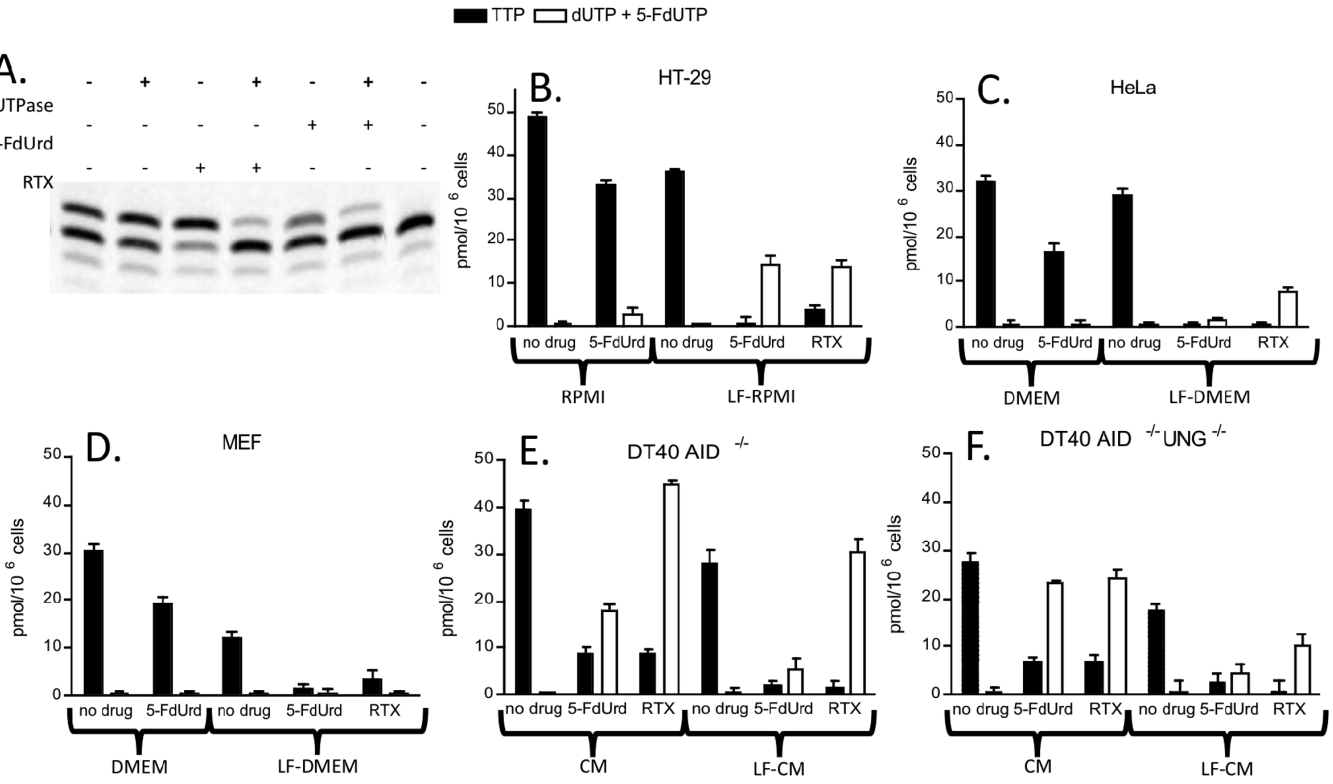

FIGURE 2: Measurement of [dUTP + 5-F-dUTP] and [TTP] in HT29, MEF, HeLa, and DT40 cell extracts in the presence and absence of 5-FdUrd (7.5 μM) and RTX (0.5 μM). (A) Denaturing polyacrylamide gel analysis of the template extension reaction using NTP extracts obtained from HT29 cells cultured in the absence and presence of 5-FdUrd using low-folate RPMI medium with dialyzed FBS. T, DNA template primer. The minor $n - 1$ band in each lane arises from pyrophosphorolysis of the template. (B–D) [TTP] and [dUTP + 5-F-dUTP] (picomoles per 10^6 cells) measured in methanol extracts obtained from HT29, HeLa, or MEF cells grown in the absence or presence of 5-FdUrd or RTX using standard or low-folate (LF) RPMI or DMEM medium. (E and F) [TTP] and [dUTP + 5-F-dUTP] (picomoles per 10^6 cells) measured in methanol extracts obtained from DT40 cells grown in the absence or presence of 5-FdUrd or RTX using standard or low-folate (LF) chicken medium (CM).

during fluoropyrimidine treatment. If the post-treatment ratio is large, then massive amounts of dUTP can be incorporated into cellular DNA during the S phase, as observed in yeast (*8*). Given the mechanistic importance of this ratio, we used a single-nucleotide extension (SNE) assay to measure the level dUTP and 5-F-dUTP and the level of TTP present in MEF, HeLa, HT-29, and DT40 cell extracts before and after treatment with 5-FdUrd and RTX (*19*). The SNE assay measures the amount of polymerase-catalyzed extension of a DNA primer/template containing a single deoxyadenosine overhang on the template strand. Thus, total TTP levels and total dUTP and 5-F-dUTP levels in a cell extract are measured in an extension reaction using this primer/template. The specific levels of TTP are obtained by pretreatment of the extracts with dUTPase, specifically converting dUTP and 5-F-dUTP to dUMP and 5-F-dUMP, respectively. The combined levels of dUTP and 5-F-dUTP are calculated as a difference, i.e., [dUTP + 5-F-dUTP] = [TTP + dUTP + 5-F-dUTP] − [TTP] (*19*) (Figure 2A).

When MEF, HeLa, or HT-29 cells were treated with 7.5 μM 5-FdUrd in standard culture medium (either DMEM or RPMI containing 10% FBS and a 1% penicillin/streptomycin mixture), we found no significant change in the combined dUTP and 5-F-dUTP levels and an only modest ~2-fold decrease in the TTP levels in the extracts (Figure 2B–D). This concentration of 5-FdUrd used in these experiments is at least 500-fold greater than its typical IC_{50} in cell culture (*7*), and these cell lines and media match those used in previous studies of glycosylase-mediated fluoropyrimidine toxicity (*7*, *9*, *10*).

5-F-dUrd and RTX Significantly Increase the dUTP/TTP Ratio When Human and Mouse Cells Are Grown in Media Containing Dialyzed FBS. Normal culture medium contains high concentrations of folate (2.5 μM) and thymidine, which could antagonize the effects of the TS drugs. Consistent with this expectation, significantly higher dUTP/TTP ratios were obtained using media containing dialyzed FBS and physiological levels of 5-methyl tetrahydrofolate (80 nM) (Figure 2B–D). Under these conditions, marked decreases in TTP levels are observed in all cell lines, and in the case of HT-29 cells, a large increase in the dUTP level occurs as well ([dUTP]/[TTP] ~ 15). The equal or greater levels of dUTP detected with RTX as compared to 5-F-dUrd strongly suggest that the majority of the uridine triphosphate pool in the presence of 5-dUrd is comprised of dUTP and not 5-F-dUTP.

Cytotoxic Effects of 5-dUrd and RTX in DT40 Chicken Cells Are Not Dependent on UNG Activity. Given the redundancy of glycosylase activities in human cells, and their complex roles in 5-FU and RTX toxicity (*7*, *9*, *10*), we turned to a simpler cell system to further elucidate the roles of dUTP pool levels and UNG in the toxicity of RTX. Chicken DT40 B cells offer several experimental advantages over the human cell lines. First, and much like yeast, DT40 cells do not have any glycosylase activity other than UNG that can remove uracil from U·A base pairs (see Figure S2 of the Supporting Information) (*20*). Second, these rapidly dividing cells spend much more time in the S phase of the cell cycle, increasing the likelihood that an S phase-specific enzyme such as UNG would play a role in the drug mechanism. Third, an *ung*$^{-/-}$ DT40 strain is available for directly

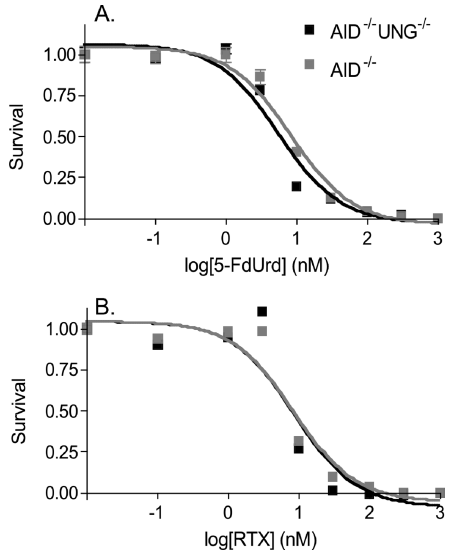

FIGURE 3: Toxicity of 5-FdUrd and RTX to DT40 cell lines that express or are deficient in UNG activity. The IC_{50} values for 5-FdUrd are 6 ± 1 nM (*aid*$^{-/-}$*ung*$^{-/-}$) and 8 ± 1 nM (*aid*$^{-/-}$) and for RTX 9 ± 2 nM (*aid*$^{-/-}$*ung*$^{-/-}$) and 8 ± 2 nM (*aid*$^{-/-}$). The error bars are standard errors from three replicate determinations.

testing the role of UNG in the absence of any other glycosylase activity. In addition, because RTX introduces only U·A base pairs into DNA, the role of mismatch repair pathways in the toxicity mechanism is expected to be absent. Thus, these cells provide a controlled system for addressing the role of UNG in repairing or precipitating the toxicity of U·A base pairs.

For comparisons using isogenic cell lines, we use the control DT40 cell line that has a knockout in the cytidine deaminase enzyme AID (*aid*$^{-/-}$), and the corresponding UNG-deficient double knockout (*aid*$^{-/-}$*ung*$^{-/-}$). The use of this strain does not impact the experimental design because the wild-type DT40 strain showed no marked difference in its response to RTX as compared to the *aid*$^{-/-}$ strain (data not shown). In general, we found that both DT40 cell lines showed a much larger increase in the dUTP/TTP ratio when treated with 5-dUrd and RTX as compared to the human cell lines, both using normal and dialyzed chicken media (Figure 2E,F). The one exception was the comparison between HeLa cells and DT40 *aid*$^{-/-}$*ung*$^{-/-}$ cells using dialyzed media, where the two cell lines responded similarly. Also, treatment with RTX resulted in greater dUTP/TTP ratios compared to those with 5-dUrd.

We measured the IC_{50} values for these drugs in normal and dialyzed chicken media using the control and UNG deletion cell lines (Figure 3). The drugs are highly active in the control strain, with an IC_{50} value of 8 ± 1 nM in normal media. The UNG deficient strain shows an IC_{50} similar to that of the control strain for both 5-dUrd and RTX (6 and 9 nM, respectively), indicating that UNG does not play a discernible protective or toxic role in the drug mechanism. Thus, even with dUTP/TTP levels as high as 30/1, and the absence of other glycosylases, a role for UNG in generating toxic abasic site lesions from 5-FU·A or U·A base pairs is not evident (see Discussion). Similar results were obtained using dialyzed chicken media.

hUNG2 Is the Primary Activity for Removal of 5-FU and U from DNA. One possible mechanism for the lack of involvement of UNG in the toxicity of 5-F-dUrd and RTX is one in which its activity level is low compared to those of other glycosidases, and/or it is poorly effective in the removal of 5-FU

Table 1: Sequences and Abbreviations of Substrates Used in This Work[a]

Substrate Abbreviation	Sequence
ssU	5′ FAM-CACTGCTCA**U**GTACAGAGC 3′
ssF	5′ FAM-CACTGCTCA**F**GTACAGAGC 3′
U/G	5′ FAM-CACTGCTCA**U**GTACAGAGC 3′ 3′ GTGACGAGT**G**CATGTCTCG 5′
U/A	5′ FAM-CACTGCTCA**U**GTACAGAGC 3′ 3′ GTGACGAGT**A**CATGTCTCG 5′
F/G	5′ FAM-CACTGCTCA**F**GTACAGAGC 3′ 3′ GTGACGAGT**G**CATGTCTCG 5′
F/A	5′ FAM-CACTGCTCA**F**GTACAGAGC 3′ 3′ GTGACGAGT**A**CATGTCTCG 5′
T/G	5′ FAM-CACTGCTCA**T**GTACAGAGC 3′ 3′ GTGACGAGT**G**CATGTCTCG 5′
C/G	5′ FAM-CACTGCTCA**C**GTACAGAGC 3′ 3′ GTGACGAGT**G**CATGTCTCG 5′

[a]Abbreviations: U, deoxyuridine; F, 5-fluorodeoxyuridine; ss, single-stranded; FAM, 6-carboxyfluorescein.

lesions. To investigate this question, we performed steady-state and single-turnover kinetic experiments with hUNG2, hSMUG1, and hTDG using substrates in which 5-FU and U were paired with A or G or were presented in the context of single-stranded DNA (Table 1), Representative steady-state and single-turnover kinetic data for hUNG2 and hSMUG1 reacting with 5-FU·A and 5-FU·G base pairs are shown in Figure 4.

Comparison of the steady-state k_{cat} values for hUNG2, hSMUG1, and hTDG[3] (Figure 5A and Table 2) shows that hUNG2 is able to process both 5-FU and U lesions at a rate at least 100-fold greater than that of either hSMUG1 or hTDG in a manner independent of the context of the lesion. Comparing activities under k_{cat}/K_m conditions, we again find that hUNG2 is superior in the excision of all substrates except for the F·G mispair, for which the k_{cat}/K_m of hUNG2 is comparable to that of hSMUG1 and 10 times slower than that of hTDG (Figure 5B and Table 2).

Because previous data for hTDG and hSMUG1 have shown that their steady-state turnover is greatly limited by the slow release of the abasic reaction product, we wanted to check their activity with hUNG2 when these enzymes were provided in excess over the DNA substrate (*14*, *15*, *21*, *22*). Thus, single-turnover measurements were performed in the presence of excess, rate-saturating amounts of hSMUG1 and hTDG. Even under very nonrealistic conditions where hSMUG1 was present at an ~200-fold greater concentration than its substrate site, its most favored substrates (U·G and F·G) were cleaved more slowly than catalytic amounts of hUNG2 (compare k_{cat} and k_{max} values in Table 2). With hTDG, single-turnover measurements show that it can excise 5-FU from a 5-FU·G base pair ~5 times faster than the k_{cat} value for hUNG (Table 2) (*14*, *15*, *22*). However, these conditions whereby [hTDG]/[S] ≫ 1 are not realistic for hTDG within the cell nucleus (see cell lysate results and Discussion). We note in this context that the k_{max} of hUNG2 for a 5-FU·G base pair is comparable to its k_{cat} because product release is not rate-limiting for the 5-FU·G substrate. Previous work has shown that the catalytic activity of hTDG correlates

[3]The kinetic properties of hTDG under solution conditions identical to those used here have been previously reported (*10*, *26*, *37*).

well with the pyrimidine leaving group pK_a (*14*). In contrast, the active sites of hSMUG1 and hUNG2 sterically preclude most C5-substituted uracil analogues (*23*, *24*). The ability of 5-FU to enter the active site of hUNG2 and hSMUG1 likely reflects the relatively small increase in the van der Waals radius of the C5 fluorine substituent of 5-FU (1.35 Å) as compared to the C5 proton substituent of U (1.20 Å).

5-FU Excision Activity of Human and Chicken Cell Extracts. Knowledge of the in vitro activity profiles of hUNG2, hSMUG1, and hTDG on 5-FU and U lesions, combined with the use of the potent and specific protein inhibitor of UNG2 (UGI), provides the experimental tools necessary to determine the relative abundance of hUNG2, hSMUG1, and hTDG in human nuclear extracts prepared in the presence and absence of a drug. In addition, similar experiments can be performed to investigate UNG activity levels in extracts prepared from *aid*$^{-/-}$ and *aid*$^{-/-}$*ung*$^{-/-}$ DT40 cells in the presence and absence of a drug.

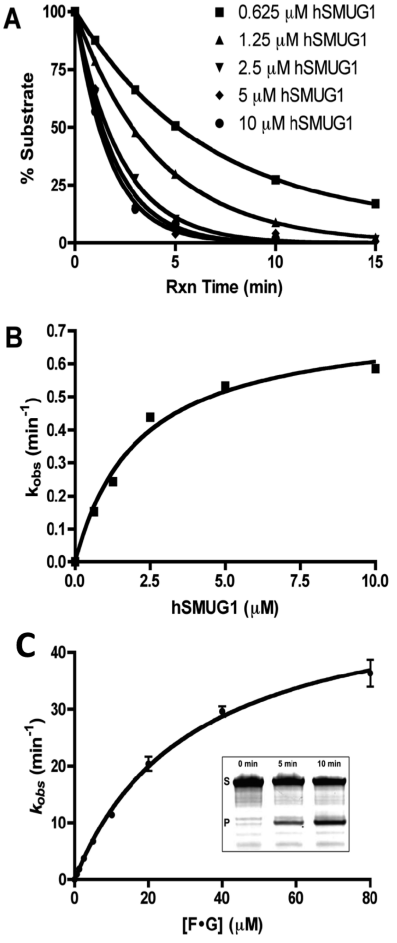

FIGURE 4: Representative single-turnover and steady-state measurements of glycosylase activity. (A) Single-turnover kinetic time courses for hSMUG1-catalyzed excision of 5-FU from the F·A duplex as a function of enzyme concentration. (B) hSMUG1 concentration dependence of the observed rate constants. The kinetic parameters are listed in Table 2. (C) Steady-state kinetics for UNG2 excision of 5-FU from the F·G duplex (Table 1). The top and bottom bands in the gel correspond to substrate and product bands, respectively.

Purified nuclei from MEF, HT-29, and HeLa cells were prepared and analyzed for their ability to excise lesions from the array of DNA substrates in Table 1. Deconvolution of the relative activity contributions of each enzyme was performed on the basis of the following rationale. First, the contribution of UNG2 to substrate cleavage can be easily assessed by performing reactions in the absence and presence of UGI (*25*). [Contrary to a previous report (*21*), we find that UGI does not inhibit either SMUG1 or TDG (Figure S3 of the Supporting Information).] Second, the specific SMUG1 activity in the extracts may be assessed from the residual ssU activity remaining in the presence of UGI, because SMUG1 is the only enzyme capable of processing ssU when UNG is inhibited (Table 2 and Figure S4 of the Supporting Information). TDG activity may be estimated from the F·A base pair activity remaining after subtraction of the contributions of both UNG2 and SMUG1 because it is the only remaining glycosylase capable of processing this lesion (Table 2) (*26*−*28*). Finally, the fractional contribution of TDG to F·G base pair excision may be estimated using its fractional contribution to F·A base pair excision (Figure S4 of the Supporting Information). The small residual F·G base pair excision activity (< 5%), after subtraction of UNG2, SMUG1, and TDG activities, may arise from MBD4.

As seen in Figure 6A−D, UNG2 is the major glycosylase activity present in nuclear extracts of MEF, HeLa, and HT-29 cell lines using substrates with F·G, F·A, and ssU lesions, regardless of whether the cell extracts were prepared from cell cultures grown in the absence or presence of 5-FU. We are able to conclude from the low levels of ssU excision in the presence of UGI that SMUG1 contributes less than 6% to the excision of 5-FU in any of the cell lines tested (Figure S4 of the Supporting Information). This finding is consistent with a previous report classifying SMUG1 as a low-abundance protein (*29*). The small SMUG1 contribution suggests that hTDG is the major processor of F·A lesions when UNG2 is absent, also agreeing with a previous study using MEF cell extracts (*10*). A lack of measurable T·G base pair excision by hTDG in these extracts is not surprising because hTDG excises F·G lesions ~2000-fold more readily than T·G lesions (*15*). Furthermore, on the basis of the relative excision activity of hTDG with F·A and F·G lesions

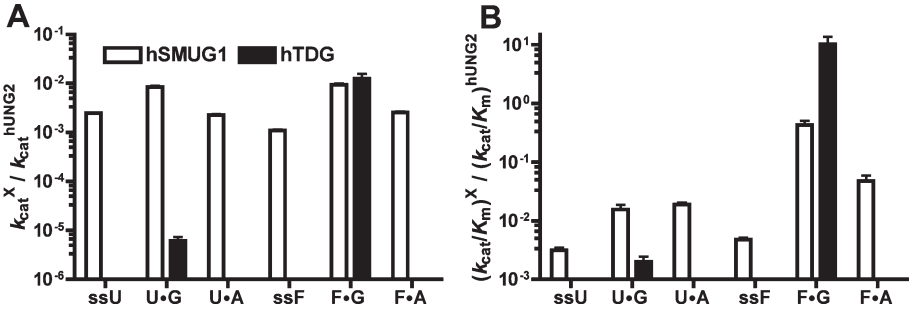

FIGURE 5: In vitro kinetic excision parameters of purified hSMUG1 and hTDG relative to hUNG2 for an array of DNA substrates. (A) k_{cat} values of hSMUG1 and hTDG relative to hUNG2. (B) k_{cat}/K_m values of hSMUG1 and hTDG relative to hUNG2. Kinetic parameters for hTDG were previously reported (*14*, *15*) under identical buffer and substrate conditions.

Table 2: Kinetic Parameters of hUNG2, hSMUG1, and hTDG on 5-FU- and U-Containing DNA Substrates[a]

	hUNG2		hSMUG1			hTDG[b]		
substrate	k_{cat} (min^{-1})	K_m (μM)	k_{cat} (min^{-1})	K_m (μM)	k_{max} (min^{-1})	k_{cat} (min^{-1})	K_m (μM)	k_{max} (min^{-1})
ssU	2193 ± 39	15 ± 1	5.6 ± 0.1	12 ± 1	≥5.6	NA	NA	NA
U·G	830 ± 30	3.3 ± 0.3	7.0 ± 0.3	1.8 ± 0.3	209 ± 16	0.005 ± 0.001	~0.01	2.2 ± 0.3
U·A	171 ± 5	3.3 ± 0.2	0.39 ± 0.01	0.40 ± 0.02	14 ± 1	ND	ND	0.0033 ± 0.0001
ssF	90 ± 4	64 ± 5	< 0.1	~10−20	ND	ND	ND	~1[c]
F·G	51 ± 2	32 ± 3	0.48 ± 0.02	0.7 ± 0.1	40 ± 6	0.63 ± 0.17	0.039 ± 0.008	278 ± 35
F·A	39 ± 2	39 ± 5	< 0.1	~1	0.7 ± 0.1	ND	ND	1.08 ± 0.08

[a]Abbreviations: ND, not determined; NA, no activity. The indicated k_{max} values are single-turnover rate constants. [b]Kinetic properties of hTDG were previously reported (*14*, *15*). [c]A. Drohat, personal correspondence, 2010.

(Figure S4 of the Supporting Information), we conclude that hTDG provides the majority of the F·G excision activity when UNG2 is absent.[4] These interpretations are not biased by the fact that steady-state catalysis by hTDG is limited by slow product release, because the addition of recombinant human apyrimidinic endonuclease to remove the inhibitory abasic product from the reactions did not alter the outcome that UNG was the predominant activity present in the extracts (Figure S6 of the Supporting Information).[5]

Given a previous report that nuclear UNG protein levels were downregulated by 5-dUrd (*30*), we compared the contribution of UNG activity in nuclear extracts prepared from cultures that had been grown with and without 1 μM 5-FU (in Figure 6, compare black and red bars). However, we did not find any measurable effect of 5-FU on the activity levels of nuclear UNG2 in these cell lines. We also measured the UNG activity in chicken cell extracts prepared in the absence and presence of 0.5 μM RTX for 24 h (Figure S2 of the Supporting Information). Similar to the results with 5-FU and human cells, no decrease in UNG activity was observed.

DISCUSSION

Reconciling the Role of DNA Glycosylases in 5-FU Toxicity. A key initial event in determining the fate of a cell during fluoropyrimidine treatment is the magnitude of the perturbations in the dUTP/TTP and 5-F-dUTP/TTP ratios (Figure 1). Mechanistically, a large increase in these ratios requires (i) efficient inhibition of thymidylate synthase, (ii) inefficient action of dUTPase and dihydropyrimidine dehydrogenase, and (iii) active nucleoside kinases. Although pyrimidine metabolism involves far more complexity than these three components, if any of these mechanistic requirements are not met, the nucleotide ratios may not be altered significantly, and the toxicity mechanism may be affected.

The mechanistic considerations mentioned above may provide an explanation for the different requirements for DNA glycosylases that have been reported in budding yeast and mammalian cell culture systems. In an UNG deletion yeast strain, genomic levels of U and 5-FU were found to be 1 per 100 and 1 per 10000 nucleotides, respectively, after treatment with 5-FU, whereas undetectable levels of uracil were found in the wild-type strain (*8*). These findings, combined with the observation that the wild-type yeast strain was 10-fold more sensitive to 5-FU than the *ung* deletion strain, require a large fluoropyrimidine-induced increase in the size of the dUTP/TTP pool in yeast, and a significant role for UNG-catalyzed uracil excision in the toxicity mechanism. In contrast, this study finds only small changes in the [dUTP + 5-F-dUTP]/TTP ratio upon treatment of three mammalian cell lines with 5-dUrd using standard cell culture medium, but much more significant increases in this ratio when using dialyzed FBS medium containing low folate levels (Figure 2). We suspect that the high folate and thymidine levels in normal medium may be strongly antagonistic to the action of fluoropyrimidines and RTX via the pyrimidine salvage pathway and direct competitive inhibition. Indeed, the consistently low dUTP/TTP ratio measured in cells grown in standard medium is fully consistent with the previously determined low levels of U and 5-FU in genomic DNA isolated from mammalian cells treated with 5-fluorodeoxyuridine. Although these genomic levels vary widely in different studies (0.01−1 uracil per 10^4 genomic nucleotides) (*9*, *10*, *13*, *31*), the levels are at least 100-fold lower than those found in yeast. Moreover, in mammalian cells, the genomic levels of 5-FU are typically detected at a density nearly 1 order of magnitude greater than that of uracil, whereas in yeast, the uracil levels greatly exceed that of 5-FU (*8*). Thus, the glycosylase-mediated toxicity of fluoropyrimidines in yeast is dominated by a large increase in dUTP levels, dense incorporation of dUTP (but not 5-F-dUTP) into DNA, UNG excision, and, ultimately, whole scale fragmentation of the yeast genome (*8*). In contrast, mammalian cells differ in two key respects. First, the large perturbation in the nucleotide pool levels never occurs in standard culture medium, and second, the level of genomic 5-FU is 1 order of magnitude higher than in yeast and even exceeds the level of genomic U. Accordingly, 5-FU cytotoxicity in MEF cells correlates more closely with the processing of 5-FU rather than U in genomic DNA (*9*, *10*).

Variable Roles of Uracil DNA Glycosylases in the Drug Mechanism. The redundancy of DNA glycosylases that act on U and 5-FU in mammalian cells leads to the possibility that the fate of these lesions may depend on the initiating glycosylase. In the case of UNG2, which we have shown is the most globally

[4]The higher ratio of U·G to F·G excision as compared to that of F·A to ssU excision in the MEF cells, but not HeLa and HT-29 extracts, suggests the presence of an increased mismatch activity. One might attribute this additional MEF mismatch activity to the mismatch-specific MBD4 glycosylase (*35*). However, because mSMUG1 has an increased mismatch activity compared to that of hSMUG1 (*36*), and the activity of MBD4 is greatly impaired at 100 mM salt (*27*), we assign this activity to mSMUG1 (see Discussion).

[5]These extract experiments overestimate the contribution of TDG activity in vivo for two reasons. First, the oligonucleotides contained 5-FU lesions in a CpG or CpA sequence context, which are preferred by TDG by 2−150-fold compared to other sequence contexts (*14*). Second, because nuclear extracts were prepared from asynchronous cell cultures, and the expression of the enzymes is cell cycle-dependent, the average amount of each enzyme present will be weighted by the fraction of the cells in each stage of the cell cycle. Because TDG is present during the G_2 and G_1 phases (> 70% of the cell cycle) and UNG2 is present in only the S phase (< 30% of the average cell cycle) (*10*, *26*, *37*), the extract preparations are weighted toward TDG.

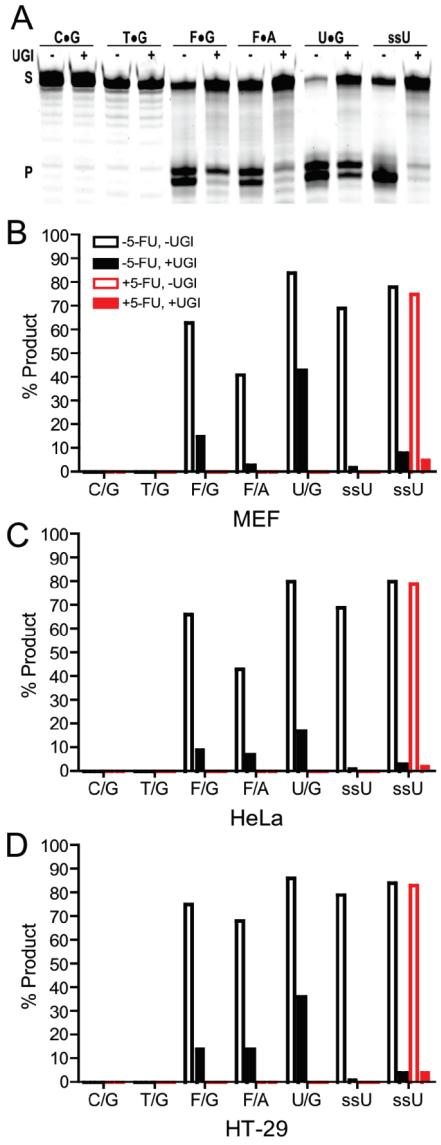

FIGURE 6: Excision of various DNA lesions by nuclear extracts obtained from cells grown in the absence (black bars) and presence (red bars) of 1 μM 5-FU for 48 h. (A) Representative gel of various DNA substrates incubated with MEF nuclear extracts in the presence and absence of the specific inhibitor of UNG (UGI). Top and bottom bands correspond to substrate (S) and product (P) bands, respectively. The identity of the central base pair of the substrate is listed above each lane (+ and − indicate the presence and absence of UGI, respectively). The two product bands are due to fractional removal of the terminal deoxyribose sugar during hot alkali processing of abasic sites. (B−D) Percent cleavage of the indicated DNA constructs from MEF, HeLa, and HT-29 cells by nuclear extracts obtained from cells grown in the absence and presence of 5-FU. Activity measurements were performed in the presence and absence of UGI to determine the contribution of UNG to the observed cleavage activity. The identical ssU activities of extracts prepared from cultures grown in the absence and presence of 5-FU indicate that UNG is not downregulated in the presence of the drug.

active uracil glycosylase in nuclear extracts, an encounter with a sparse uracil or 5-FU residue during S phase DNA replication is easily repaired given the abundance and activity of the enzyme. Unlike the yeast system, these UNG-initiated repair events may not be sufficiently dense to elicit fork arrest or double-strand breaks, and accordingly, UNG activity does not precipitate drug toxicity. The low levels of U and 5-FU that escape detection of UNG during the S phase are then intercepted during the G_1 or G_2 phase by the redundant activity of SMUG1, accounting for the fluoropyrimidine hypersensitivity of SMUG1 deficient cells (*9*). Finally, the encounter of a 5-FU·G lesion by TDG appears to be cytotoxic, based on the decrease in fluoropyrimidine sensitivity of cells where TDG activity has been knocked down using RNA silencing. These results suggest that lesion excision by TDG during the G_1 or G_2 phase results in faulty repair, DNA strand breaks, or the initiation of an apoptotic signaling pathway.

Consistent with the idea that the identity of the initiating repair glycosylase can determine a lesion's fate, it is not surprising that mismatch repair (MMR) is strongly implicated in exerting 5-FU cytotoxicity (*6*, *32*, *33*). Unlike uracil BER, which excises and replaces only a single damaged nucleotide, MMR recognition of a 5-FU·G or U·G mismatch directs a DNA nick ~250−1000 bp from the mismatch by a complex of MMR proteins (*11*). The entire length of the DNA strand from the nick to the mismatch is then degraded and synthesized anew, increasing the chances of incorporating a new lesion during the repair process. In a manner independent of this futile repair cycle, MMR has also been shown to exert 5-FU cytotoxicity via the signaling of cell cycle arrest and apoptosis during lesion detection (*28*).

The report that hUNG is downregulated in many, but not all, human cell lines during treatment with 5-dUrd adds an additional layer of complexity to the understanding of the drug mechanism (*30*). This downregulation could represent a survival strategy in some transformed cell lines that allows evasion of what would be an otherwise toxic effect of uracil residues introduced during S phase DNA synthesis. Consistent with this idea, HeLa cells do not show this same hUNG2 downregulation and are protected against the toxicity of 5-dUrd when hUNG2 is silenced using siRNA methods (*30*). This effect with 5-dUrd is not recapitulated in our studies using 5-FU or RTX in the same cell lines, as well as in chicken cells. These apparently conflicting results may reflect significant differences in the cellular response to 5-FU and RTX as opposed to 5-dUrd.

The Toxicity of 5-dUrd and RTX to DT40 Cells Is Independent of Uracil BER and MMR. The DT40 chicken cell line provides a useful system for exploring the relative role of uracil excision repair and mismatch repair in the toxicity mechanisms of 5-dUrd and RTX. The similar IC_{50} values of these drugs, the lack of involvement of UNG, and the similar perturbations in dUTP and TTP with both drugs strongly suggest a common cell killing mechanism that may be related to the perturbation in the nucleotide pool levels. Moreover, a significant involvement of MMR in the toxicity mechanism is not indicated because 5-FdUrd should activate this pathway through the incorporation of 5-F-dUTP, while RTX (which produces only dUTP) should not. These results in DT40 cells are most consistent with the original thymineless death mechanism for fluoropyrimidine action.

Implications for Cancer Therapy. The different cytotoxic mechanisms of fluoropyrimidines in yeast, mammalian, and chicken cells suggest that the pathway for cell killing might be pharmacologically selected with appropriate compounds. The variable results with different TS inhibitors and different cell types suggest that it will be difficult to predict the clinical outcome for a given tumor and drug without knowledge of the pathways that are involved. Selection of a different killing pathway would be beneficial if a tumor is defective in a DNA repair pathway that is otherwise required for the cytotoxic effect. One established example is MMR deficient colon cancers that are resistant to 5-FU (*33*). If the killing mechanism could be switched to a

UNG-dependent killing pathway (as observed in HeLa cells), the efficacy of the drug might be restored. One possible approach to this end would be to inhibit the enzyme dUTPase, which can lead to large increases in dUTP levels during fluoropyrimidine treatment (*34*). Such perturbations could shift the toxicity mechanism to one that involves UNG, as already observed in yeast.

ACKNOWLEDGMENT

We thank Dr. Alexander Drohat for the TDG enzyme used in these studies.

SUPPORTING INFORMATION AVAILABLE

Six supporting figures. This material is available free of charge via the Internet at http://pubs.acs.org.

REFERENCES

1. Longley, D. B., Harkin, D. P., and Johnston, P. G. (2003) 5-Fluorouracil: Mechanisms of Action and Clinical Strategies. *Nat. Rev. Cancer 3*, 330–338.
2. Wyatt, M. D., and Wilson, D. M. (2009) Participation of DNA Repair in the Response to 5-Fluorouracil. *Cell. Mol. Life Sci. 66*, 788–799.
3. Van Triest, B., Pinedo, H. M., Giaccone, G., and Peters, G. J. (2000) Downstream Molecular Determinants of Response to 5-Fluorouracil and Antifolate Thymidylate Synthase Inhibitors. *Ann. Oncol. 11*, 385–391.
4. Cohen, S. S. (1971) On the Nature of Thymineless Death. *Ann. N.Y. Acad. Sci. 186*, 292–301.
5. Houghton, J. A., Tillman, D. M., and Harwood, F. G. (1995) Ratio of 2′-Deoxyadenosine-5′-triphosphate/thymidine-5′-Triphosphate Influences the Commitment of Human Colon Carcinoma Cells to Thymineless Death. *Clin. Cancer Res. 1*, 723–730.
6. Carethers, J. M., Chauhan, D. P., Fink, D., Nebel, S., Bresalier, R. S., Howell, S. B., and Boland, C. R. (1999) Mismatch Repair Proficiency and in Vitro Response to 5-Fluorouracil. *Gastroenterology 117*, 123–131.
7. Andersen, S., Heine, T., Sneve, R., König, I., Krokan, H. E., Epe, B., and Nilsen, H. (2005) Incorporation of dUMP into DNA is a Major Source of Spontaneous DNA Damage, while Excision of Uracil is Not Required for Cytotoxicity of Fluoropyrimidines in Mouse Embryonic Fibroblasts. *Carcinogenesis 26*, 547–555.
8. Seiple, L., Jaruga, P., Dizdaroglu, M., and Stivers, J. T. (2006) Linking Uracil Base Excision Repair and 5-Fluorouracil Toxicity in Yeast. *Nucleic Acids Res. 34*, 140–151.
9. An, Q., Robins, P., Lindahl, T., and Barnes, D. E. (2007) 5-Fluorouracil Incorporated into DNA is Excised by the Smug1 DNA Glycosylase to Reduce Drug Cytotoxicity. *Cancer Res. 67*, 940–945.
10. Kunz, C., Focke, F., Saito, Y., Schuermann, D., Lettieri, T., Selfridge, J., and Schär, P. (2009) Base Excision by Thymine DNA Glycosylase Mediates DNA-Directed Cytotoxicity of 5-Fluorouracil. *PLoS Biol. 7*, e91.
11. Fischer, F., Baerenfaller, K., and Jiricny, J. (2007) 5-Fluorouracil is Efficiently Removed from DNA by the Base Excision and Mismatch Repair Systems. *Gastroenterology 133*, 1858–1868.
12. Krokan, H. E., Drabløs, F., and Slupphaug, G. (2002) Uracil in DNA: Occurrence, Consequences and Repair. *Oncogene 21*, 8935–8948.
13. Luo, Y., Walla, M., and Wyatt, M. D. (2008) Uracil Incorporation into Genomic DNA does Not Predict Toxicity Caused by Chemotherapeutic Inhibition of Thymidylate Synthase. *DNA Repair 7*, 162–169.
14. Morgan, M. T., Bennett, M. T., and Drohat, A. C. (2007) Excision of 5-Halogenated Uracils by Human Thymine DNA Glycosylase. Robust Activity for DNA Contexts Other than CpG. *J. Biol. Chem. 282*, 27578–27586.
15. Fitzgerald, M. E., and Drohat, A. C. (2008) Coordinating the Initial Steps of Base Excision Repair. Apurinic/apyrimidinic Endonuclease 1 Actively Stimulates Thymine DNA Glycosylase by Disrupting the Product Complex. *J. Biol. Chem. 283*, 32680–32690.
16. Jiang, Y. L., Krosky, D. J., Seiple, L., and Stivers, J. T. (2005) Uracil-Directed Ligand Tethering: An Efficient Strategy for Uracil DNA Glycosylase (UNG) Inhibitor Development. *J. Am. Chem. Soc. 127*, 17412–17420.
17. Lee, K. A., Bindereif, A., and Green, M. R. (1988) A Small-Scale Procedure for Preparation of Nuclear Extracts that Support Efficient Transcription and Pre-mRNA Splicing. *Gene Anal. Tech. 5*, 22–31.
18. Horowitz, R. W., Zhang, H., Schwartz, E. L., Ladner, R. D., and Wadler, S. (1997) Measurement of Deoxyuridine Triphosphate and Thymidine Triphosphate in the Extracts of Thymidylate Synthase-Inhibited Cells using a Modified DNA Polymerase Assay. *Biochem. Pharmacol. 54*, 635–638.
19. Horowitz, R. W., Zhang, H., Schwartz, E. L., Ladner, R. D., and Wadler, S. (1997) Measurement of Deoxyuridine Triphosphate and Thymidine Triphosphate in the Extracts of Thymidylate Synthase-Inhibited Cells using a Modified DNA Polymerase Assay. *Biochem. Pharmacol. 54*, 635–638.
20. Di Noia, J. M., Rada, C., and Neuberger, M. S. (2006) SMUG1 is Able to Excise Uracil from Immunoglobulin Genes: Insight into Mutation Versus Repair. *EMBO J. 25*, 585–595.
21. Kavli, B., Sundheim, O., Akbari, M., Otterlei, M., Nilsen, H., Skorpen, F., Aas, P. A., Hagen, L., Krokan, H. E., and Slupphaug, G. (2002) HUNG2 is the Major Repair Enzyme for Removal of Uracil from U:A Matches, U:G Mismatches, and U in Single-Stranded DNA, with hSMUG1 as a Broad Specificity Backup. *J. Biol. Chem. 277*, 39926–39936.
22. Bennett, M. T., Rodgers, M. T., Hebert, A. S., Ruslander, L. E., Eisele, L., and Drohat, A. C. (2006) Specificity of Human Thymine DNA Glycosylase Depends on N-Glycosidic Bond Stability. *J. Am. Chem. Soc. 128*, 12510–12519.
23. Kavli, B., Slupphaug, G., Mol, C. D., Arvai, A. S., Peterson, S. B., Tainer, J. A., and Krokan, H. E. (1996) Excision of Cytosine and Thymine from DNA by Mutants of Human Uracil-DNA Glycosylase. *EMBO J. 15*, 3442–3447.
24. Nilsen, H., Rosewell, I., Robins, P., Skjelbred, C. F., Andersen, S., Slupphaug, G., Daly, G., Krokan, H. E., Lindahl, T., and Barnes, D. E. (2000) Uracil-DNA Glycosylase (UNG)-Deficient Mice Reveal a Primary Role of the Enzyme during DNA Replication. *Mol. Cell 5*, 1059–1065.
25. Wang, Z., and Mosbaugh, D. W. (1989) Uracil-DNA Glycosylase Inhibitor Gene of Bacteriophage PBS2 Encodes a Binding Protein Specific for Uracil-DNA Glycosylase. *J. Biol. Chem. 264*, 1163–1171.
26. Hardeland, U., Bentele, M., Jiricny, J., and Schar, P. (2000) Separating Substrate Recognition from Base Hydrolysis in Human Thymine DNA Glycosylase by Mutational Analysis. *J. Biol. Chem. 275*, 33449–33456.
27. Petronzelli, F., Riccio, A., Markham, G. D., Seeholzer, S. H., Stoerker, J., Genuardi, M., Yeung, A. T., Matsumoto, Y., and Bellacosa, A. (2000) Biphasic Kinetics of the Human DNA Repair Protein MED1 (MBD4), a Mismatch-Specific DNA N-Glycosylase. *J. Biol. Chem. 275*, 32422–32429.
28. Meyers, M., Wagner, M. W., Mazurek, A., Schmutte, C., Fishel, R., and Boothman, D. A. (2005) DNA Mismatch Repair-Dependent Response to Fluoropyrimidine-Generated Damage. *J. Biol. Chem. 280*, 5516–5526.
29. Nilsen, H., Haushalter, K. A., Robins, P., Barnes, D. E., Verdine, G. L., and Lindahl, T. (2001) Excision of Deaminated Cytosine from the Vertebrate Genome: Role of the SMUG1 Uracil-DNA Glycosylase. *EMBO J. 20*, 4278–4286.
30. Fischer, J. A., Muller-Weeks, S., and Caradonna, S. J. (2006) Fluorodeoxyuridine Modulates Cellular Expression of the DNA Base Excision Repair Enzyme Uracil-DNA Glycosylase. *Cancer Res. 66*, 8829–8837.
31. Canman, C. E., Lawrence, T. S., Shewach, D. S., Tang, H. Y., and Maybaum, J. (1993) Resistance to Fluorodeoxyuridine-Induced DNA Damage and Cytotoxicity Correlates with an Elevation of Deoxyuridine Triphosphatase Activity and Failure to Accumulate Deoxyuridine Triphosphate. *Cancer Res. 53*, 5219–5224.
32. Meyers, M., Wagner, M. W., Hwang, H. S., Kinsella, T. J., and Boothman, D. A. (2001) Role of the hMLH1 DNA Mismatch Repair Protein in Fluoropyrimidine-Mediated Cell Death and Cell Cycle Responses. *Cancer Res. 61*, 5193–5201.
33. Li, L. S., Morales, J. C., Veigl, M., Sedwick, D., Greer, S., Meyers, M., Wagner, M., Fishel, R., and Boothman, D. A. (2009) DNA Mismatch Repair (MMR)-Dependent 5-Fluorouracil Cytotoxicity and the Potential for New Therapeutic Targets. *Br. J. Pharmacol. 158*, 679–692.
34. Koehler, S. E., and Ladner, R. D. (2004) Small Interfering RNA-Mediated Suppression of dUTPase Sensitizes Cancer Cell Lines to Thymidylate Synthase Inhibition. *Mol. Pharmacol. 66*, 620–626.
35. Bellacosa, A. (2001) Role of MED1 (MBD4) Gene in DNA Repair and Human Cancer. *J. Cell. Physiol. 187*, 137–144.
36. Pettersen, H. S., Sundheim, O., Gilljam, K. M., Slupphaug, G., Krokan, H. E., and Kavli, B. (2007) Uracil-DNA Glycosylases SMUG1 and UNG2 Coordinate the Initial Steps of Base Excision Repair by Distinct Mechanisms. *Nucleic Acids Res. 35*, 3879–3892.
37. Hengst, L., and Reed, S. I. (1996) Translational Control of p27Kip1 Accumulation during the Cell Cycle. *Science 271*, 1861–1864.